International Journal of Research Publication and Reviews

Journal homepage: www.ijrpr.com ISSN 2582-7421

Developing a Renewable Energy and Controller-Based Power Management System for Electric Vehicles

K. Siva Ganesh

PG Scholar, Dept. of EEE, Bonam Venkata Chalamayya Engineering College, Odalarevu, INDIA

ABSTRACT:

This paper discusses the design process of a bidirectional Dc-DC converter for EV battery charging systems which includes power management implementation. The bidirectional flow capability of the bidirectional DC-DC converter allows its widespread use in EV battery charging systems combined with DC microgrid (DCMG) applications. The design of PV-battery-fed DCMG requires a SEPIC converter to stabilize DC bus voltage. The vector controller together with the DC side controllers operate efficiently in steady-state and transient-state conditions through proper controllers for battery charging and discharging operations. Using EPS modulation extends the connection between the vector controller and dc side controllers converter with the specified DCMG for power transmission to an EV battery while preventing back power flow. This designed system can undergo additional analysis through closed-loop operation of vector controller and DC side controllers for bi-directional power flow.

Keywords: Energy Management System; Renewable energy; Electric Vehicle.

I. Introduction

A worldwide concern surrounds global warming as the climate rises annually alongside increasing planet-warming gases including CO2 and sulphur and others. Conservative fuel-powered vehicles which use petrol alongside diesel engines contribute substantially to this problem of pollution. Researchers undertake studies of diverse energy options because people worldwide focus on pollution reduction and climate preservation [1-2]. The collaboration between governments and leading automobile companies aims to create realistic methods for reducing fossil fuel utilization which reduces automotive carbon emissions because vehicles have become a primary polluting factor. EV development stands as the most effective method to decrease automotive CO2 emissions [2].

A significant number of electric vehicle products have existed and been used worldwide since the late 19th century. The latest innovations exist as either long-term prototypes or concepts for automotive vehicles or function as single-use models. The discovery of new battery-powered EV vehicles marks an industry milestone starting from late 19th century. Although lithium-ion and Li-ion batteries displaced the newer technology at some point the lithium-ion battery remains price-to-power dominant. Lithium-ion batteries appear in electric vehicles because of their widespread application.

New hybrid electric cars using conventional engines stand as various options in the market. The car leads to environmental impact due to its engine costs while also causing pollution. The only automated energy source available at present for battery-powered electric vehicles operates through the motor. The new appropriate controller enables electric cars to function with both AC and DC motors [2-4]. Among the determinants for motor selection stand the cost, performance, size, efficiency of the motor and its control mechanism. The use of electric vehicle (EV) motors presents different advantages and disadvantages between each type. High-power capacity requires heavy and economically affordable alternating current motors but their performance relies heavily on using the correct induction motor controller.

BLDC and PMSM together with induction and switching reluctance motors (SRM) represent the electric motor technology employed in electric vehicles (EEV). The control torque function in EVs originates from the driving machine itself. The control system needs both quick reactions and low motor torque fluctuations in order to function properly. A high-performance electric motor coupled with a broad speed range must be implemented for EV applications. The integration of AC motors enables us to decrease both the machine range and its price. Electric vehicles have one main drawback because they possess restricted battery storage capacity. The amount of driving distance an EV can handle depends on its capability to obtain available battery power.

II. Proposed Design

a. Selection of System Components:

EVs and HEVs depend on four basic components that include vehicle arrangement combined with battery-based systems and motor DC-DC converters and control mechanisms. Standard weight requirements for the carried passengers must be assumed by the vehicles. We utilized the mass of the mentioned equipment to decide sizes as well as ratings for both the components and the strategy. Reference [5] provided the methodology for body vehicle weight measurement. The references suggest [5, 6] that the body weight measurement should include the engine weight and comes in at approximately 1500 kg. The below section presents estimated dimensions and ratings for the components.

b. Calculation Power base on Motor Dynamics:

Testing all systematic resistances in combination with grade resistances and aerodynamic forces ensures proper identification of the required motor power rating for the proposed HEVS. The measurement for HEVS's total weight stands at 1500 kg according to figure 1. This paper requires proper definition of all its parameters.

The necessary force for dynamic a vehicle's is designed below [5]:

$$F_{total} = FR + F_{gradient} + F_{aerodynamic} \tag{1}$$

Where, F_{total} =Total force in vechile

F_R= force due to Resistance Rolling;

$F_{gradient}$ = force due to ResistanceGradient;

$F_{aerodynamic}$= force due to drag aerodynamic.

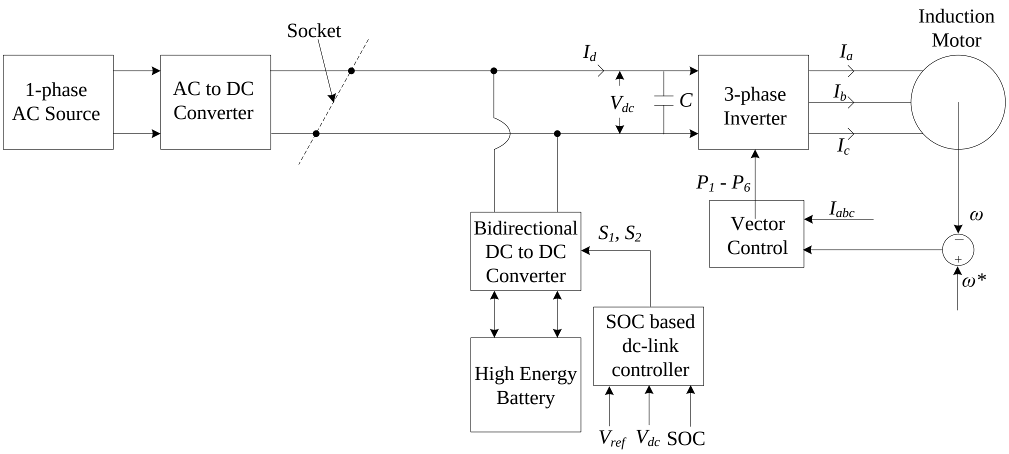

Fig.1: Proposed System in Hybrid Electric Vehicle

c. Modeling of the Battery:

Electric automobiles and cell phones together with TV remote controls and various electrical devices function through batteries that are electrochemical systems made from one or more electrochemical cells. People preference rechargeable batteries because such technology enables multiple cycles of discharge and recharging through applied electric current. The amount of electric charge during normal use determines the capacity of a battery system. At normal temperature the 100 Ah battery can discharge power continuously at 5A for 20 hours.

Any Electric Vehicle (EV) and Hybrid Electric Vehicle (HEV) contains a battery system which represents its highest expense. For batteries to reach their optimal service duration the charging method and discharge procedures need close management. The primary responsibility of battery management systems in electric cars is to perform this function. The EV or complete HEV battery extends its voltage output through multiple linked battery units arranged in series. Throughout the charging process, the same current passes through each element. The battery chain life increases through equal charge distribution across cells by maintaining voltage stability in each element. Each battery element may possess different quantities of source resistance but will maintain equivalent tolerance levels. The different voltages each element receives create damage potential.

The measurement results allow the computation of both state of health (SOH) and state of charge (SOC) values which get recorded. The research uses a generalized battery model from its original appearance in [13]. For more precise battery modeling the temperature parameter is considered within the system. The model system utilizes a basic regulated voltage source combined with a constant resistance as illustrated in Figure 2.

Where the controlled voltage source is described through below equations,

$$E_m = E_{m0} - K_E(273 + \theta)(1 - SOC) \tag{2}$$

$$Q_e(t) = Q_{e\_init} + \int_0^t - I_m(\tau)d\tau \quad (3)$$

$$I_p = V_{PN} G_{P0} \exp\left(\frac{V_{PN}}{V_{P0}(\tau_P s + 1)} + A_P\left(1 - \frac{\theta}{\theta_f}\right)\right) \quad (4)$$

$$C(I,\theta) = \frac{K_c C_{0*} K_t}{1 + (K_c - 1)(I/I^*)^{\delta}}, \; K_t = LUT(\theta) \quad (5)$$

$$SOC = 1 - \frac{Q_e}{C(0,\theta)}, \quad DOC = 1 - \frac{Q_e}{C(I_{avg},\theta)}, \quad \theta(t) = \theta_{init} + \int_0^t \frac{\left(Ps - \frac{(\theta - \theta_a)}{R_\theta}\right)}{C_\theta} d\tau$$

Where,

Where, E_m is the open-circuit voltage (V), E_{m0} is the open circuit voltage at full charge (V), θ is electrolyte temperature (^{0}C), Q_e is the extracted charge (A S), $Q_{e_init}$is the initial extracted charge (A S), I_m is the main branch current (A), τ is an integration time variable, I_P is the current loss in parasitic branch, V_{PN} is the voltage at the parasitic branch, τ_P is a parasitic branch time constant, θ_f is electrolyte freezing temperature (^{0}C), C_{0*} is the no-load capacity at 0^0C, K_t is a temperature dependent look-up table, I^* is a nominal battery current, DOC is a depth of charge, C is the battery capacity (A) , K_E, G_{P0} and δ are constants.

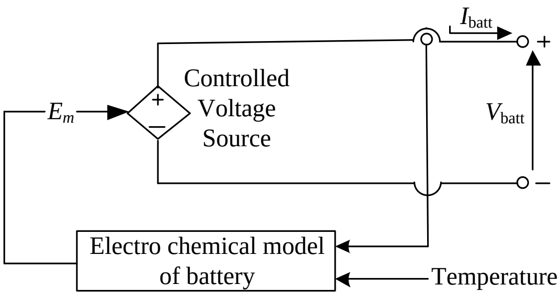

Fig. 2: Generic Battery Model

An illustration of how an HEV system should be configured appears in Figure 3. The traction motor requires AC power from the figure depicted. The battery, a DC source, serves as the primary electrical power source. The DC link voltage management process requires that the battery sends its DC output to a DC-to-DC bidirectional converter which performs voltage boosting or bucking. The DC output becomes AC through the operation of a vector-controlled PWM inverter. Right sequencing of gating pulses allows the inverter to generate AC power from DC while controlling both voltage level and frequency.

Ideal inverters employing PWM modulation will generate sinusoidal signals when the output connects to correct LC filter networks. Harmonics and essentially non-sinusoidal outputs still occur though the inverter generates them. An appropriate energy management system alongside DC-to-DC converters functions according to [1-2, 13, 21-23] and literary sources 1 and 2.

d. Bidirectional DC-DC Converter:

An innovative bidirectional power flow results from the bidirectional DC to DC converter that operates successfully between the high-voltage DC bus and low-voltage battery [1, 10]. A state of charge (SoC)-based controller serves to increase battery lifespan according to figure 3. To achieve the required charging/discharging current specifications the DC link voltage operates between specific limits. The operation modes of bidirectional DC to DC converters include plug-in AC/DC battery charging and the battery-to-EV bus boost operation and the high voltage-to-battery buck operation for regenerative charging.

A bidirectional DC to DC converter enables the connection of battery voltage to the DC link. The bidirectional converter enables lower reference DC link voltage (V*dc) compared to battery voltage thus facilitating connected batteries in parallel with less number of cells. This suggested system has battery voltage at 300 V while V*dc equals 526 V stands for the high energy battery rating with consideration of 90% depth of discharge (DOD). A modified version of hysteresis band control uses the controller's output signal to specify the reference current for the battery in order to switch S1 or S2 of the bidirectional converter.

The control signal provides a specific range where it stops to maintain actual battery charging and discharging current levels according to design specifications. The DC link voltage should remain beyond the minimum value needed to produce the required motor voltage.

The battery system will automatically disconnect from charging when its state of charge reaches 95%. The PI controller accepts DC-link voltage measurement as its input error signal. The PI controller generates battery current references which depend on the current DC voltage level at the reference side. Voltage on the DC connection will undergo fluctuations when there is a power imbalance. The reference battery current will be transformed into pulses through the hysteresis band since it operates by comparing real battery current with reference current. The pulse signals will activate the switches and control the converter's bidirectional DC to DC duty cycle operation. The controller included the SOC to lengthen the battery lifetime. A detailed depiction of the controller circuit exists in Figure 4.

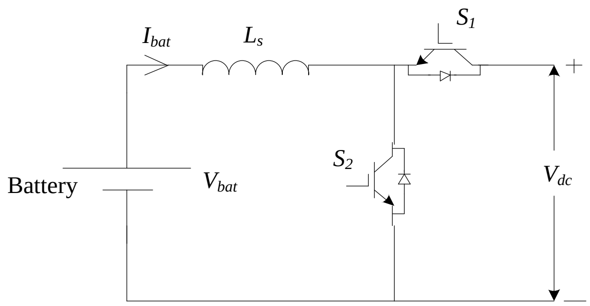

Fig. 3: Bidirectional DC to DC Converter

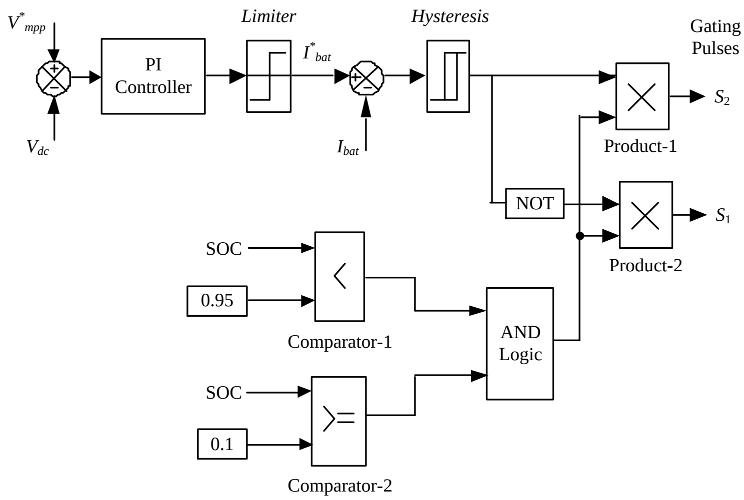

Fig.4: DC to DC converter control

III. Proposed System and Control Design

a. Change in Load Torque:

The motor receives a nominal load torque of 5 Nm at t=1.5 seconds and it increases to Nm at t=3 seconds. The battery needs to supply enough power to the motor to prevent decreasing the available charging power from the power supply combined with motor usage. Under steady state operations the vector control system helps generate electromagnetic torque to deliver or achieve the reference torque needed to drive the system without speed variations.

The responses shown in Figures 5 and 6 correspond to one another as they display torque and speed data. The data from Fig. 6 reveals that motor speed reaches equilibrium while maintaining a constant torque delivery. Speed decreased throughout the transient period because of the methods used to counter electromagnetic torque and load torque. The vector control system works to stabilize motor reference speed under changing torque conditions. The matching currents and battery power diagram is presented in Figures 7 and 8.

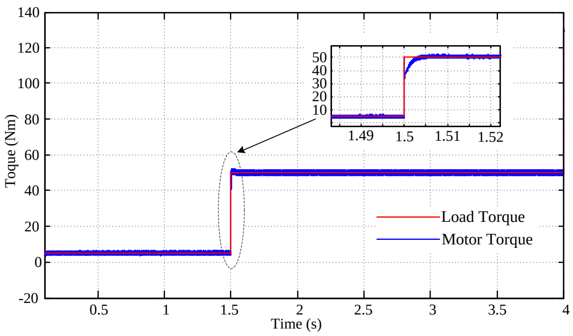

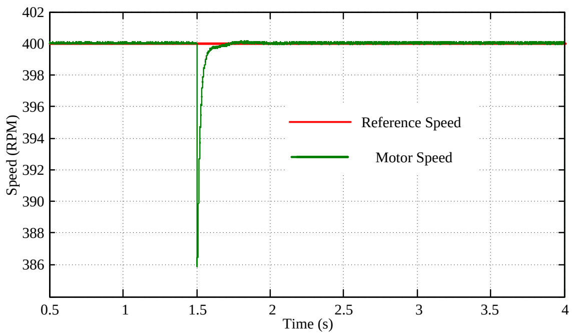

Fig. 5: Load and electromagnetic torque generated by Motor; Fig. 6: Response of Speed under Increasing Load Torque

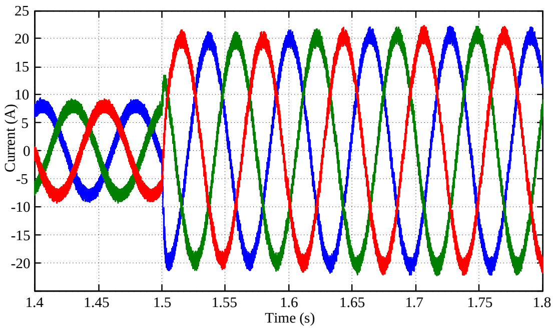

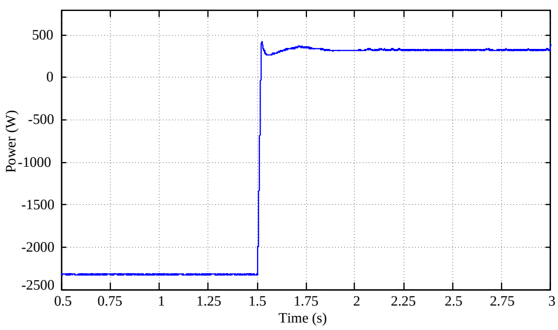

Fig.7: Line currents of Induction motor under change in torque; Fig. 8: Battery power under charging and discharging mode for changing in load torque

The MATLAB Simulink program implemented for the suggested system performed simulations which are displayed in Fig. 9. The calculated flux position θ depends on all mathematical formulas which appeared in parts 1 and 2. The θ value leads to the generation of the sine and cosine unit vectors cosθ and sinθ. The vector controller determines appropriate motor currents by using the rotor frame but establishes the three-phase motor currents by using the stator frame [1-4]. Multiple equations derived from previous sections enable this transformation to change stator currents between stationary and synchronous reference frames. A controller receives two components namely command torque and flux current as its main inputs.

The stator current components in direct and synchronous quadrature frames (iqse and ides) receive comparison against the controller inputs. The system undergoes tests within multiple operational conditions. The subsequent section provides acceptable analysis results and satisfactory outcomes for the case studies. This section displays the necessary criteria as well as the ratings that follow the case study analysis. The system operates at 524 V Vmpp with a 10 horsepower motor under 1000 W/m2 irradiance delivering 2798 W maximum power output. The vehicle runs at 50 km/h, each tire extends 2.08 meters and requires 400 RPM motor speed for 178 Nm torque generation while using Matlab R2013a software and 300V battery power. The rating of battery current stands at 100 Ah and hysteresis current stretches from 1.5A to 1.5A.The results are carried out by considering below possibilities.

1. Working under maximum power from PV (Change in solar irradiance)
2. Change in Speed (with constant torque)
3. Change in torque (with constant speed)
4. Reverse Speed (required to run a car in reverse direction)

The results are briefly examined and explained by following cases.

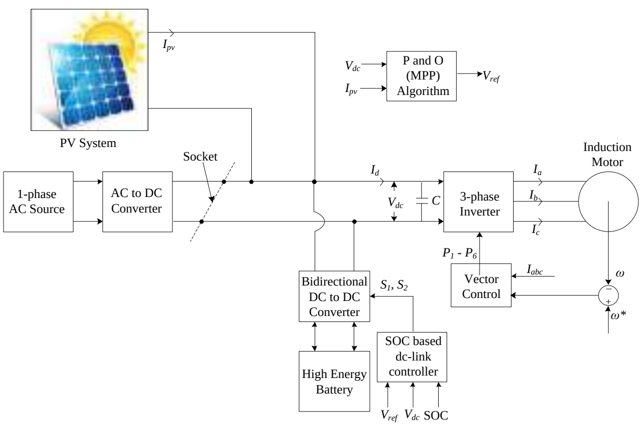

Fig. 9: Proposed System in Hybrid Electric Vehicle

IV. Results and Discussions

a. System performance under change in solar irradiance:

Figure 10 illustrates how the system applied the radiation decrease from 1000 W/m2 to 700 W/m2 at the time point t=3 sec. The P and O control method will track the voltage at maximum power (Vmpp) as the irradiance reaches 700 W/m2 for this specific situation. The profiles of PV curves appear across multiple irradiance levels in Part 2 of the figure (Fig. 10). Based on Fig. 10 in part 2 of the document the P and O algorithm delivers the proper voltage at maximum power for irradiance at 700 W/m2 before transmitting it to a bidirectional DC to DC converter controller. The converter sustains Vmpp as the reference value which regulates Vdc. The equivalent results for Vmpp and Vdc are displayed in Fig. 11 and Fig. 12 shows the maximum output of the PV system. Through the use of P and O algorithm the DC-to-DC converter controller functions as an MPPT converter for the PV system.

A reduction in solar irradiation causes output loss in the induction motor which prompts the battery to discharge energy to sustain constant speed. The induction motor will experience constant current drawing at t = 3 seconds because the battery maintains power equilibrium. The speed of hybrid electric automobiles remains unaffected by solar conditions and passenger count so these factors should be irrelevant. The vehicle maintains its reference speed without speed variations regardless of sudden changes in sun irradiation. The necessary element to achieve this power balancing is an adjustable DC to DC controller operating in bidirectional mode. The matching battery power together with the currents and speed measurements for the induction motor are displayed in Figures 13, 14, and 15. Load torque stays constant in this particular analysis. The PV achieves adequate power alongside satisfactory speed, current, voltage and performance levels at the point of its maximum power rating. The controllers demonstrate operational efficiency according to the results obtained in this case. The controllers together with the system operate perfectly throughout both transient and steady-state operational conditions as confirmed by satisfiable test results. The specific speed value of this induction motor reaches 400 RPM which equals to 50 Kmph.

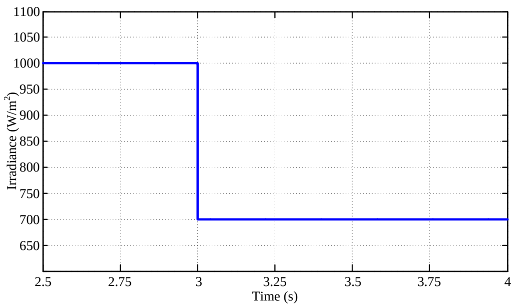

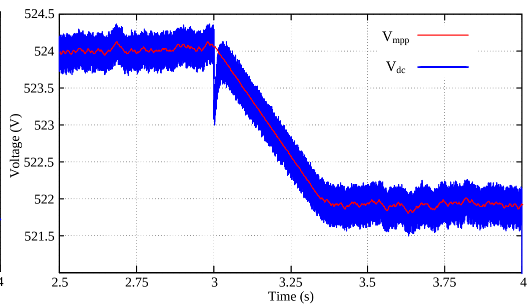

Fig. 10: Change in Solar Irradiance; Fig. 11: Response of reference (Vmpp) and dc link voltage (Vdc)

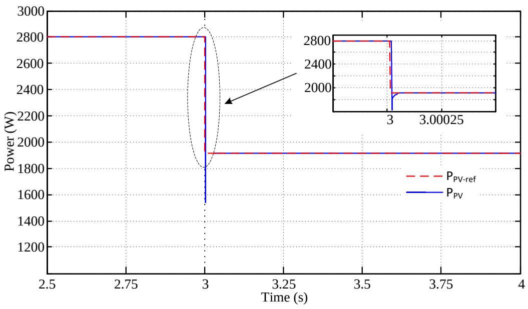

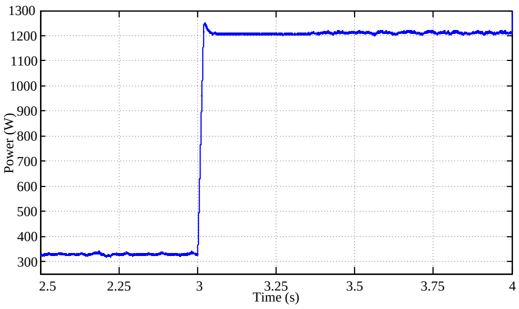

Fig. 12: Output power of PV system; Fig. 13: Battery power (Discharging mode)

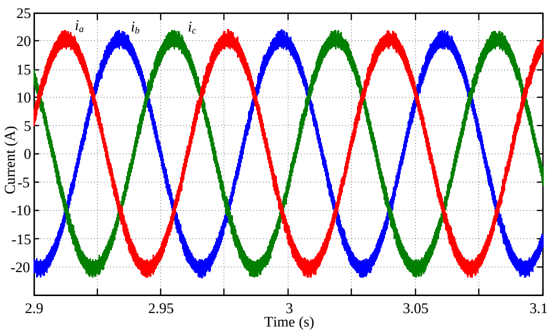

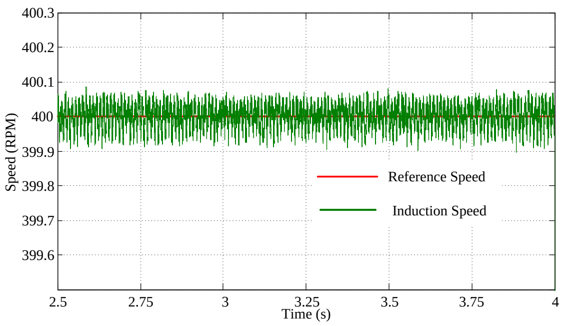

Fig. 14: line currents of Induction motor; Fig. 15: Speed of the Induction motor

V. Conclusion

The above mentioned case studies demonstrate that the vector controller with DC side controllers function appropriately throughout steady-state as well as transient-state conditions. The system performance tests were conducted through MATLAB Simulink software since we faced hardware limitations. The case studies show how the proposed controllers deliver uninterrupted driving operation.

References

[1]. Tirupati Uttamrao Solanke et al., “A review of strategic charging–discharging control of grid-connected electric vehicles”, Journal of Energy Storage, Vol. 28, 2020.

[2]. Aqueel A., Zeeshan A., Khan, M., Saad A., Siddique K., “A review of the electric vehicle charging techniques, standards, progression and evolution of EV technologies in Germany,” J. Smart Sci., Vol. 1, Issue. 6, 2018.

[3]. Y. Sun, C. Jiang, Z. Wang, L. Xiang, H. Zhang, Bi-directional wireless power transfer for vehicle-to-grid systems, Korea Institute Power Electron. Vol. 18-4, 2018.

[4]. Ricardo J. Bessa and Manuel A. Matos, “Economic and technical management of an aggregation agent for electric vehicles: a literature survey”, European Transactions on Electrical Power, 2012.

[5]. Gaizka Saldaña, et. al., “Electric Vehicle into the Grid: Charging Methodologies Aimed at Providing Ancillary Services Considering Battery Degradation”, Energies, Vol. 12, 2019.

[6]. Tugrul U. Daim, Xiaowen Wang, Kelly Cowan and Tom Shott, “Technology roadmap for smart electric vehicle-to-grid (V2G) of residential chargers”, Journal of Innovation and Entrepreneurship, Vol. 5, Issue 15, 2016.

[7]. W. Shireen and S. Patel, S., “Plug-in hybrid electric vehicles in the smart grid environment,” inProc. of IEEE PES Transmission and Distribution Conference and Exposition,pp. 1-4, Apr. 2010.

[8]. Siddhartha, M., Arunabh, C., Albert, Y., & Rajit, G. (2012). Electric vehicle smart charging and vehicle-to-grid operation. International Journal of Parallel, Emergent and Distributed Systems, 27, 3.

[9]. Smart, John, Jamie Davies, Matthew Shirk, Casey Quinn, and Kenneth S. Kurani, 2010, “Electricity demand of PHEVs operated by private households and commercial fleets: effects of driving and charging behavior”, [Online] Availableat: http://avt.inel.gov/pdf/phev/EVS25_INL_UCDavis.pdf (accessed March 2011).

[10]. SPINNOVATION, 2012. “Using fleets of electric vehicles for electric power grid support”, [Online], Available at: http://www.lifepo4.info/ Battery_study/V2G_memo_Senter_V02.pdf.

[11]. Rücker, F.; Bremer, I.; Linden, S.; Badeda, J.; Sauer, D.U. Development and Evaluation of a Battery Lifetime Extending Charging Algorithm for an Electric Vehicle Fleet. Energy Proced. 2016, 99, 285–291.

[12]. Ruecker, F.; Bremer, I.; Sauer, D.U. Development and analysis of a charging algorithm for electric vehicle fleets extending battery lifetime. In Proceedings of the ITEC-AP, Busan, South Korea, 1–4 June 2016; p. 29.

[13]. Hu, X.; Zou, Y.; Yang, Y. Greener plug-in hybrid electric vehicles incorporating renewable energy and rapid system optimization. Energy 2016, 111, 971–980.

[14]. Wu, H.; Pang, G.K.; Choy, K.L.; Lam, H.Y. A charging-scheme decision model for electric vehicle battery swapping station using varied population evolutionary algorithms. Appl. Soft Comput. 2017, 61, 905–920.

[15]. Kempton W, Tomic J. Vehicle-to-grid power fundamentals: calculating capacity and net revenue. Journal of Power Sources 2005; 144:268–279. DOI: 10.1016/j.jpowsour.2004.12.025.

[16]. Kempton W, Tomic J. Vehicle-to-grid power implementation: from stabilizing the grid to supporting large-scale renewable energy. Journal of Power Sources 2005; 144:268–279. DOI: 10.1016/j.jpowsour.2004.12.022.